





[View Journal Online](#)
[View Article Online](#)

Highly efficient fluorescence resonance energy transfer in co-encapsulated BODIPY nanoparticles

 Priyadarshine Hewavitharanage *, Launa Steele  and Isaac Dickenson 

 Department of Chemistry, University of Southern Indiana, Evansville, Indiana 47712, USA
phewavitha@usi.edu (P.H.), lgsteele@eagles.usi.edu (L.S.), igdickenso@eagles.usi.edu (I.D.)

 * Corresponding author at: Department of Chemistry, University of Southern Indiana, Evansville, Indiana 47712, USA.
 e-mail: phewavitha@usi.edu (P. Hewavitharanage).

RESEARCH ARTICLE



doi: 10.5155/eurjchem.12.4.361-367.2155

 Received: 18 July 2021
 Received in revised form: 20 August 2021
 Accepted: 28 August 2021
 Published online: 31 December 2021
 Printed: 31 December 2021

KEYWORDS

 Encapsulation
 Amphiphilic polymer
 Polymer nanoparticles
 Fluorescence enhancement
 Boron-dipyrromethene (BODIPY)
 Fluorescence resonance energy transfer

ABSTRACT

Fluorescence resonance energy transfer (FRET) is a powerful tool used in a wide range of applications due to its high sensitivity and many other advantages. Co-encapsulation of a donor and an acceptor in nanoparticles is a useful strategy to bring the donor-acceptor pair in proximity for FRET. A highly efficient FRET system based on BODIPY-BODIPY (BODIPY: boron-dipyrromethene) donor-acceptor pair in nanoparticles was synthesized. Nanoparticles were formed by co-encapsulating a green emitting BODIPY derivative (FRET donor, $\lambda_{\max} = 501$ nm) and a red emitting BODIPY derivative (FRET acceptor, $\lambda_{\max} = 601$ nm) in an amphiphilic polymer using the precipitation method. Fluorescence measurements of encapsulated BODIPY in water following 501 nm excitation caused a 3.6 fold enhancement of the acceptor BODIPY emission at 601 nm indicating efficient energy transfer between the green emitting donor BODIPY and the red emitting BODIPY acceptor with a 100 nm Stokes shift. The calculated FRET efficiency was 96.5%. Encapsulated BODIPY derivatives were highly stable under our experimental conditions.

 Cite this: *Eur. J. Chem.* 2021, 12(4), 361-367

 Journal website: www.eurjchem.com

1. Introduction

Fluorescence energy transfer occurs when a high energy absorbing fluorophore (donor, D) transfers its excitation energy to a nearby low energy absorbing chromophore (acceptor, A) in its ground state through a non-radiative process. Fluorescence energy transfer can occur through bond or through space. When the donor and the acceptor are linked through a twisted conjugated spacer, through bond energy transfer predominates [1-3]. Through-space energy transfer known as fluorescence resonance energy transfer (FRET) or Förster energy transfer occurs through long-range dipole-dipole interactions between the donor-acceptor pair [4-6]. FRET does not require a physical contact or interaction between the donor and the acceptor molecule. However, the rate of FRET depends on (i) the extent of overlap between the donor emission spectrum and the acceptor absorption spectrum, (ii) the relative orientation of the donor emission and the acceptor excitation dipoles, (iii) the separation between the donor and the acceptor (typically 10-100 Å), and (iv) the fluorescence quantum yield of the donor [7-10]. Extreme sensitivity of FRET to D-A separation distance allows utilization of FRET in monitoring a variety of biological processes that cause changes in molecular proximity. It has been extensively

used in biosensing and nano-sensing applications [11,12]. FRET has been used in monitoring protein-protein interactions [13], drug-protein interactions [14], DNA-protein interactions [15], conformational changes in protein [16], receptor-mediated endocytosis [17], and drug release [18]. Due to high sensitivity and low-cost, FRET is a powerful tool for biomedical imaging [19,20].

A wide variety of organic dyes such as naphthalene, pyrene, coumarin, rhodamine, Nile Red, and Boron-dipyrromethene (BODIPY) have been utilized in FRET systems [4,21,22]. Among all, the small fluorophore, BODIPY has received significant attention due to its superior photophysical properties. Their highly fluorescent quantum yields, high extinction coefficients, chemical and photo stability and their feasible synthesis and functionalization makes them attractive candidates for FRET. Electrical neutrality of the BODIPY molecule, insensitivity to pH and solvent polarity are additional advantages for biological applications [23,24]. BODIPY has been extensively studied for many applications such as labeling of biomolecules, imaging, laser dyes, solar cells, chemical sensors, fluorescent indicators and probes, and ion sensors [25,26]. BODIPY based donor/acceptor systems such as energy transfer cassettes and artificial light harvesting arrays are also reported [1,27,28].

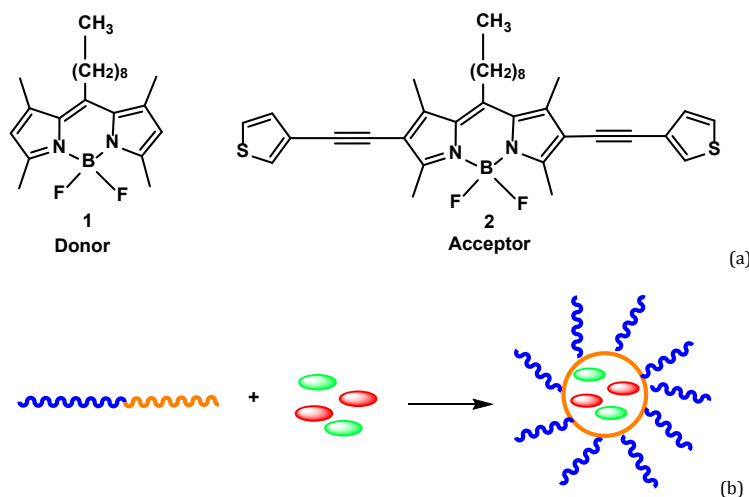


Figure 1. (a) Structures of BODIPY **1** and **2**; (b) Schematic diagram of Co-encapsulation of BODIPY **1** (Green) and **2** (Red) using an amphiphilic polymer (blue: hydrophilic portion, yellow: hydrophobic portion).

Most of the organic dyes (including BODIPY) are hydrophobic in nature. However, many biological and biomedical applications require water soluble fluorescence dyes that are compatible with the aqueous biological environment. Attaching hydrophilic groups has been used to increase water solubility. Nevertheless, it is often synthetically challenging, and purification of such compounds is difficult [29]. In addition, such groups often decrease fluorescence intensities [30]. Encapsulation of the fluorophores in amphiphilic polymers has emerged as a feasible strategy for this problem [22,31,32]. In spite of its potential, only few examples of co-encapsulated systems for FRET have been reported. For example, an enzyme-responsive theranostic FRET Probe with 88% FRET efficiency was made using curcumin/Nile red D-A system with an amphiphilic polyester [22]. Poly(lactic-co-glycolic acid) nanoparticles encapsulating BODIPY (Donor) and Nile Red (Acceptor) with ~70% FRET efficiency is reported [33]. Artificial light-harvesting assemblies with a BODIPY molecule coupled with bacteriochlorin acceptor resulting greater than 90% FRET efficiency is also known [34]. In all these systems BODIPY fluorophore is used as the donor.

In a previous study, we reported highly efficient energy transfer in an asymmetric dimeric BODIPY [1]. Arrangement of the BODIPY units in the dimers were investigated by DFT calculations. Perpendicular arrangement of BODIPY core breaks the conjugation between two BODIPY units which enables donor-acceptor behavior with efficient excitation energy transfer [1]. However, the synthesis and purification of these dimers are highly time consuming and often gives a poor yield. In addition, due to the hydrophobic nature, they need to be dissolved in a carrier solvent such as DMSO for biological studies. DMSO has some cytotoxic effect and limits biomedical applications of these molecules [35]. Hence, we seek to investigate the possibility of bringing two individual BODIPY molecules in proximity to facilitate FRET. Our strategy in this study is to utilize an amphiphilic polymer DSPE-PEG₅₀₀₀ for noncovalent encapsulation of the BODIPY donor and the acceptor. DSPE-PEG is a widely used biocompatible, biodegradable amphiphilic polymer [36] and self-assembly of the polymer will produce a hydrophobic core encapsulating BODIPY dyes while the hydrophilic corona will make it water soluble (Figure 1b). We selected two BODIPY molecules previously synthesized in our lab, a green emitting BODIPY (λ_{max} emission = 498 nm) with high quantum yield as the donor and an orange-red emitting BODIPY (λ_{max} emission = 600 nm) as the acceptor. Because the high fluorescence quantum yield of

the donor and the emission spectrum of the donor overlaps well with the absorption of the acceptor, we expect efficient energy transfer between them. We hypothesized that coprecipitating D and A with the polymer will produce encapsulated nanoparticles to bring D and A in proximity for FRET. Nonyl substituent on the meso position of the BODIPY core of D and A increases the hydrophobicity which further helps to localize BODIPY in the hydrophobic core. To the best of our knowledge, polymer encapsulated FRET systems with BODIPY/BODIPY donor-acceptor pair has not been reported.

2. Experimental

2.1. Materials

DSPE-PEG₅₀₀₀ was purchased from Laysan Bio, Inc. and used as received. Solvents used for synthesis of compounds **1** and **2** were purified using standard purification methods [37].

2.2. Instrumentation

UV-Visible spectra were recorded using a Cary 5000 Series UV-VIS-NIR spectrophotometer. Fluorescence spectra were recorded using a Horiba Jobin Yvon Fluoromax-4 spectrofluorometer.

2.3. Photophysical properties

The fluorescence spectra of compounds **1** and **2** in THF were recorded by exciting compound **1** at 489 nm and compound **2** chromophores at 563 nm. Slit width was kept at 1 nm both at the excitation and emission. The width of slits and other data collection parameters were kept the same for each measurement. The FRET data were obtained by exciting co-encapsulated dyes at 501 nm, and the emission was collected at 489-750 nm range. FRET efficiency was calculated using Equation (1). Ratiometric FRET was calculated by dividing the emission intensity of the acceptor at 601 nm by the emission intensity of the donor at 501 nm.

$$\text{FRET} = 1 - \frac{\text{Fluorescence intensity of the donor}}{\text{Fluorescence intensity of the free donor}} \quad (1)$$

2.4. Synthesis

2.4.1. Synthesis of **1** and **2**

Compounds **1** and **2** were synthesized as previously reported [38].



Figure 2. (a) The visual colors of 1:1 molar mixture of BODIPY **1**, **2** before encapsulation (green) and after encapsulation (orange) at 365 nm using a hand-held UV lamp. (b) SEM image of co-encapsulated nanoparticles.

5, 5-Difluoro-1, 3, 7, 9-tetramethyl-10-nonyl-5H-4λ⁴, 5λ⁴-dipyrrolo[1,2-c:2',1'-f][1,3,2]diazaborinine (1): ¹H NMR (300 MHz, CDCl₃, δ, ppm): 6.07 (s, 2H, indacene-H), 2.96 (t, *J* = 8.0 Hz, 2H, CH₂), 2.51 (s, 6H, 2CH₃), 2.40 (s, 6H, 2CH₃), 1.62 (br m, 2H, CH₂), 1.48 (br m, 2H, CH₂), 1.27 (br s, 10H, 5CH₂), 0.87 (t, *J* = 6.6 Hz, 3H, CH₃). ¹³C NMR (75 MHz, CDCl₃, δ, ppm): 153.8 (2C, indacene-C), 146.8 (1C, indacene-C), 140.4 (2C, indacene-C), 131.5 (2C, indacene-C), 121.6 (2C, indacene-C), 32.0 (2C, 2CH₃), 30.5 (2C, 2CH₃), 29.6 (1C, CH₂), 29.5 (1C, CH₂), 29.3 (1C, CH₂), 28.6 (1C, CH₂), 22.7 (2C, 2CH₂), 16.4 (1C, CH₂), 14.5 (1C, CH₂), 14.1 (1C, CH₃).

5,5-Difluoro-1,3,7,9-tetramethyl-10-nonyl-2, 8-bis(thiophen-3-ylethynyl)-5H-4λ⁴, 5λ⁴-dipyrrolo[1, 2-c:2', 1'-f][1, 3, 2]diazaborinine (2): ¹H NMR (400 MHz, CDCl₃, δ, ppm): 7.43 (dd, *J* = 6.4, 1.6 Hz, 2H, Ar-H), 7.28 (q, *J* = 0.007 Hz, 2H, Ar-H), 7.17 (dd, 6.4 Hz, 1.2 Hz, 2H, Ar-H), 2.65 (s, 6H, 2CH₃), 2.53 (s, 6H, 2CH₃), 1.62 (br m, 2H CH₂), 1.49 (br m, 2H CH₂), 1.27 (br m, 12H, 6CH₂), 0.87 (t, *J* = 6.8 Hz, 3H, CH₃). ¹³C NMR (100 MHz, CDCl₃, δ, ppm): 156.9 (2C, indacene-C), 147.7 (1C, indacene-C), 141.2 (2C, indacene-C), 131.4 (2C, indacene-C), 129.9 (2C, indacene-C), 128.3 (2C, Ar-C), 125.5 (2C, Ar-C), 122.5 (2C, Ar-C), 116.3 (2C, Ar-C), 91.3 (2C, ethynyl-C), 81.3 (2C, ethynyl-C), 31.9 (1C, CH₂), 30.5 (2C, 2CH₃), 29.6 (2C, 2CH₃), 29.3, (1C, CH₂), 28.7, (1C, CH₂), 22.8, (1C, CH₂), 15.3, (1C, CH₂), 14.2, (1C, CH₂), 13.8. (1C, CH₃).

2.4.2. Fluorescence quantum yield (Φ) measurements in THF:

Fluorescence quantum yield (Φ) for each compound was determined on a series of dilute solutions with absorbance values between 0.02 and 0.08 at the excitation wavelength given in Table 1. The relative fluorescence quantum yield (Φ_s) was determined as:

$$\Phi_s = \Phi_{st} \left(\frac{I_s}{I_{st}} \right) \left(\frac{A_{st}}{A_s} \right) \left(\frac{\eta_{2s}}{\eta_{2st}} \right) \quad (2)$$

where Φ is a fluorescence quantum yield, η represents the refractive index of the solvent used for the measurement, subscripts *s* and *st* represent the samples and the external standards, *I* is the integrated fluorescent intensity and *A* is the absorbance at the excitation wavelength. Rhodamine B was used as the reference ($\Phi = 0.65$ in ethanol).

2.4.3. Synthesis of co-encapsulated **1** and **2**

Co-encapsulation of **1** and **2** were performed using the coprecipitation method. Stock solutions of **1** and **2** were prepared in THF. A 226 μ mol solution of DSPE-PEG₅₀₀₀ was prepared in water. A 31 μ mol THF solution of BODIPY **1** was combined with 31 μ mol THF solution of **2**. Then 880 μ L of this combined THF solution of **1** and **2** was added to 120 μ L of DSPE-PEG₅₀₀₀ (226 μ mol solution in water) to achieve 1:1:1 molar ratio of **1**:**2**:DSPE-PEG₅₀₀₀. The resulting mixture (1 mL) was rapidly injected into a vial containing 10 mL of deionized water using a syringe. The mixture was then sonicated for 5 min. The

vial containing the mixture was placed in a 45 °C water bath. THF was removed by blowing argon on the surface of the solution. The resulting solution (2.73×10^{-5} mol/L) of **1** and **2** was filtered through 0.2 μ m Whatman® Anotop® 25 syringe filter. SEM image was taken by drop casting 2.73×10^{-5} mol/L aqueous solution on a glass slide and evaporation of water by blowing argon.

2.4.4. Determination of stability of nanoparticles

The polymer co-encapsulated suspension was incubated for 7 days at room temperature. Stability of aggregates was monitored by measuring fluorescent intensity of the donor and acceptor at different time points and calculating the ratiometric FRET.

3. Results and discussion

3.1. Synthesis and encapsulation

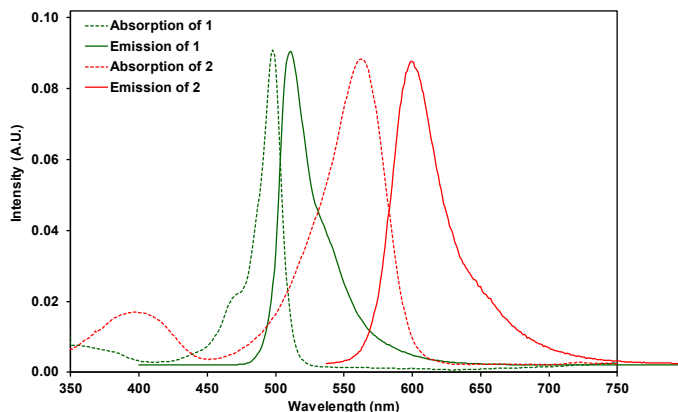
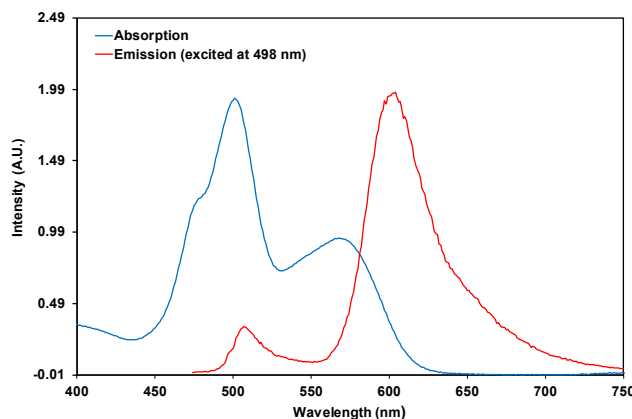
Dyes **1** and **2** were synthesized as described in our previous publication³⁶ and characterized by NMR, UV/Vis and their fluorescence spectra. Several attempts of encapsulation were performed to determine the ratio of **1**:**2**:DSPE-PEG₅₀₀₀ to achieve the optimal energy transfer and 1:1:1 molar ratio was the optimal. A solution of free **1** and **2** (before encapsulation) appeared light pink in color under ambient light and the bright green fluorescence was observed under 365 nm UV lamp (Figure 2). Injecting the solution of compounds **1**, **2** and the polymer into 10 mL water and evaporation of THF changed the fluorescence from green to red due to formation of BODIPY encapsulated polymer nanoparticles (Figure 2). Self-assembly of the polymer localizes hydrophobic BODIPY **1** and **2** in the core which brings them in proximity for FRET (Figure 1b). As expected, the SEM image of nanoparticles shows spherical morphology.

3.2. Photophysical properties

The UV-Vis absorption and fluorescence experiments were carried out in THF using a Cary 5000 Series UV-VIS-NIR Spectrophotometer. Similar to our previous photophysical data in CH₂Cl₂ [39], compounds **1** and **2** show typical BODIPY absorption bands (Figure 3), the more prominent, lowest energy absorption band due to the S₀-S₁ (π - π^*) transition and the weaker absorption band, ~350-430 nm which is more prominent in compound **2**, is due to the S₀-S₂ (π - π^*) transition (Figure 3) [1,39]. Absorption maximum of the BODIPY **2** which has ethynylthiophene units at the 2,6 positions is a 65 nm redshifted in comparison to compound **1** (Table 1). These values are almost identical in THF and CH₂Cl₂ (Table 1). Substantial overlap of the emission spectrum of compound **2** with the absorption spectrum of compound **1** satisfies the spectral overlap requirement for FRET (Figure 3) [7-10].

Table 1. Photophysical properties of compounds **1** and **2** in CH₂Cl₂ and THF^a.

Compound	Absorbance λ_{\max} (nm)	Emission λ_{\max} (nm)	Stokes shift	Quantum yield (%)
1	498 ^b , 501	504 ^b , 512	6 ^b , 11	84 ^b , 85
2	563	595 ^b , 601	32 ^b , 38	34 ^b , 32

^a Rhodamine B was used as reference ($\phi = 65\%$ in ethanol).^b In CH₂Cl₂ [39].**Figure 3.** Normalized Absorption and emission spectra of BODIPY **1** (Green) and **2** (Red) in THF.**Figure 4.** Normalized (to the acceptor emission peak) absorption (blue) and emission upon 501 nm excitation (red) spectra of co-encapsulated BODIPY **1**, **2** in water.

According to [Figure 3](#), there is a slight overlap of the normalized absorption spectra of compounds **1** and **2** which can cause simultaneous excitation of both chromophores. This may lead to slight overestimation of the energy transfer efficiency. However, in unnormalized absorption spectra, the intensity at 501 nm of compound **2** is only 1.7% of the intensity of compound **1** which is negligible when considering the high quantum yield of compound **1**. BODIPY **1** has small Stokes shift (6 nm, 14 nm) because geometry of the S₁ state of compound **1** is very similar to that of the ground state [1]. A small Stokes shift is undesirable due to reabsorption of emitted photons and which leads to decreased intensity and background interference. BODIPY **2** with 2,6 thienyl substituted BODIPY molecules has relatively larger Stokes shifts (32 nm, 38 nm). Absorption λ_{\max} of co-encapsulated donor and the acceptor are identical to those of the free donor (**1**) and the acceptor (**2**) while Emission λ_{\max} of the donor and the acceptor are 508 and 601 nm, respectively ([Figure 4](#)). Lack of splitting or red shifting of the spectral bands confirms the absence of stacking or formation of aggregates. Quantum yield of fluorescence in CH₂Cl₂ and THF were almost identical ([Table 1](#)). Spectra of individually encapsulated **1** and **2** at 3×10⁻⁵ mol/L concentration are identical to those of free compounds **1** and **2**.

3.3. Fluorescence resonance energy transfer

Emission spectra provided information about donor/acceptor energy transfer taking place in these encapsulated molecules. Considering the high fluorescence quantum yield of the donor and the considerable overlap between the emission spectrum of the donor and the absorption spectrum of the acceptor, we anticipated efficient energy transfer between compounds **1** and **2** in co-encapsulated particles. Excitation of 1:1 mixture of compounds **1** and **2** in THF at 501 nm resulted in high intensity emission at 512 nm corresponding to emission of compound **1** ([Figure 5](#)). Absence of emission by compound **2** following 501 nm excitation conformed that there is no energy transfer between solvent separated compounds **1** and **2**. Excitation of co-encapsulated mixture at the same wavelength caused a sharp decrease in donor emission at 512 nm with an emission band at 601 nm corresponding to the acceptor emission giving 100 nm pseudo-Stokes shift. This is a clear visual evidence of FRET between compounds **1** and **2** ([Figure 5](#)). Most of the fluorescent dyes have small Stokes shifts which increase background noise and complicate spectral resolution. Having a large Stokes shift is highly advantageous for applications such as fluorescence imaging. Excitation of the donor at different wavelengths is given in [Figure 6](#).

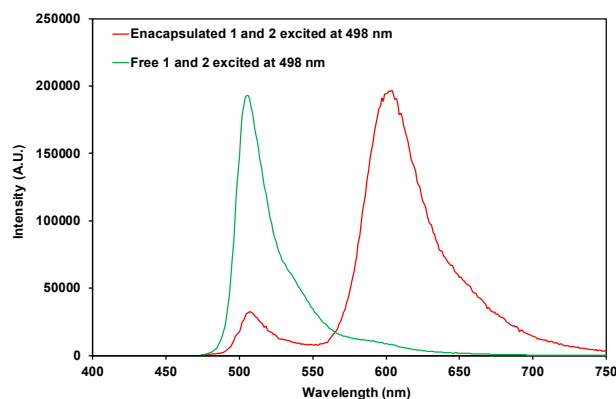


Figure 5. Green: Normalized (to the acceptor emission peak) emission spectrum of a mixture of compounds **1** and **2** (3×10^{-5} mol/L) in THF Green: before encapsulation (Excited at 501 nm), Red: Emission of co-encapsulated **1** and **2** (3×10^{-5} mol/L) in water (excited at 501 nm).

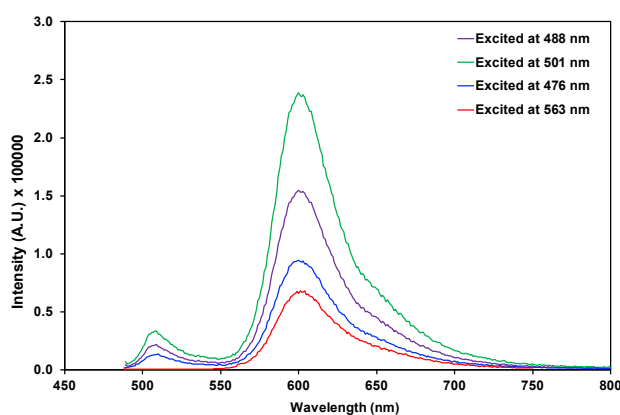


Figure 6. Emission followed by excitation of compound **1** at different wavelengths.

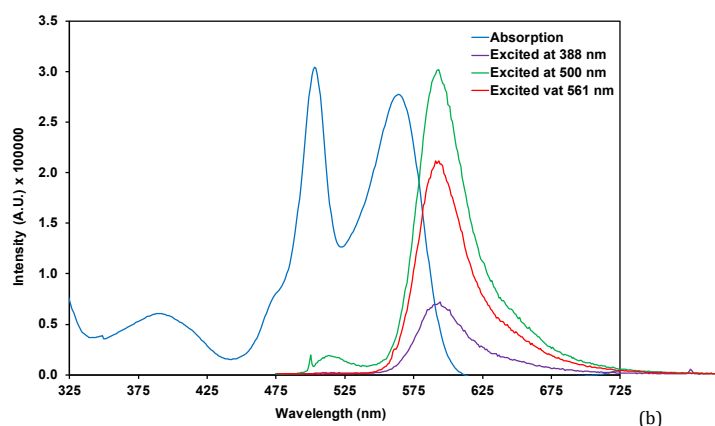
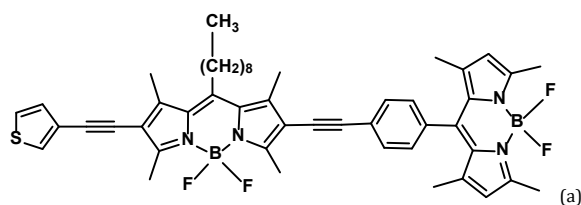


Figure 7. Structure of the BODIPY dimer (a) and its emission followed by excitation at different wavelengths (b) [1].

The highest emission intensities for both donor and the acceptor were observed upon 501 nm excitation. Intensity of the 476 nm excitation (shoulder of the absorption spectrum of compound **1**, Figure 6) was much lower. Selective excitation of the acceptor at 563 nm resulted in a single peak corresponding

to the acceptor emission ($\lambda_{\text{max}} = 601$ nm, Figures 5 and 6). Interestingly, the intensity of the acceptor emission followed by all three excitations (501, 488, and 476 nm) were higher than that of 563 nm excitation. Intensity of the 601 nm emission followed by 501 nm excitation is a 3.6-fold enhancement com-

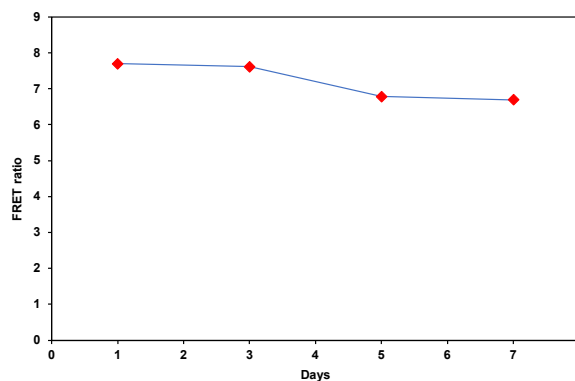


Figure 8. FRET ratio plot at different measurement time points.

pared to 563 nm excitation. It was 2.3-fold and 1.4-fold enhancement with respect to 488 and 476 nm excitations. This agrees with the results of our previous study of the dimer that was composed of two chromophores similar to BODIPY 1 and 2 (Figure 7) [1]. DFT calculations on the dimer suggest that excitation of the donor at λ_{\max} produces S_0 - S_2 transition, and the fluorescence enhancement is due to efficient S_2 - S_1 internal conversion following high intensity S_0 - S_2 excitation [1]. Similar emission enhancement has been observed between BODIPY (donor)- and Nile Red (acceptor) [34]. Energy transfer efficiency was calculated using equation 2 and found to be 96.4 % which is very close to the that of the dimer [1]. Donor/acceptor intensity ratio (ratiometric FRET) was calculated by dividing the emission intensity of acceptor by the emission intensity of donor and was found to be 7.7 for 501 nm excitation (Equation 1). In the dimer where the donor and the acceptor are covalently linked, produced 97.3% efficiency of energy transfer [1].

3.4. Stability of co-encapsulated 1 and 2

Stability of nanoparticles is crucial for their applications. Recovery of the donor intensity and decreased acceptor emission intensity are indications of reduced energy transfer between the D-A pair due to dye leaking or degradation of particles. The polymer co-encapsulated suspension was incubated at room temperature for 7 days. Stability of particles was monitored by measuring the fluorescent intensity of the donor and the acceptor at different time points. Reporting ratiometric FRET is advantageous rather than reporting change in intensity of the acceptor, because the ratio is independent of the absolute concentration of the sensor, hence effect of solvent evaporation upon storage can be eliminated. The FRET ratio was changed from 7.7 to 6.9 which is just a 13% change for one week indicating high stability.

4. Conclusion

In summary, we have engineered a novel and highly efficient FRET system by careful selection of a donor and an acceptor with high stability, substantial spectral overlap, and a donor with high fluorescence quantum yield. We selected a green emitting BODIPY 1 as the donor and an orange red emitting BODIPY 2 as the acceptor. Energy transfer was facilitated by convenient co-encapsulation of them in an amphiphilic polymer in water. Excitation of the donor resulted in emission by the acceptor with 96.5% FRET efficiency producing large pseudo-Stokes shift. This is very close to the efficiency of the dimer we previously synthesized connecting a BODIPY donor and an acceptor with similar structures. This confirms the effectiveness of encapsulation in developing FRET

probes without complicated and time-consuming synthetic routes. Fluorescence measurements of encapsulated BODIPY in water indicated substantial (3.6-fold) enhancement of the acceptor emission. Encapsulated BODIPY derivatives were quite stable at room temperature. Due to the nontoxic nature of BODIPY, superior photophysical properties, high FRET efficiency, and stability, this co-encapsulated FRET system is an excellent candidate for a FRET probe for chemical, physical, biological, and biomedical applications.

Acknowledgment

Authors acknowledge Thomas Hardin and Red Spot Paint & Varnish Co., Evansville, IN for the SEM measurements.

Disclosure statement

Conflict of interests: The authors declare that they have no conflict of interest.

Ethical approval: All ethical guidelines have been adhered.


Sample availability: Samples of the compounds are available from the author.

CRedit authorship contribution statement

Conceptualization: Priyadarshine Hewavitharanage; Methodology: Priyadarshine Hewavitharanage; Software: Priyadarshine Hewavitharanage, Launa Steele, Isaac Dickenson; Validation: Priyadarshine Hewavitharanage, Launa Steele, Isaac Dickenson; Formal Analysis: Priyadarshine Hewavitharanage, Launa Steele, Isaac Dickenson; Investigation: Priyadarshine Hewavitharanage, Launa Steele, Isaac Dickenson; Resources: Priyadarshine Hewavitharanage; Data Curation: Priyadarshine Hewavitharanage, Launa Steele, Isaac Dickenson; Writing - Original Draft: Priyadarshine Hewavitharanage; Writing - Review and Editing: Priyadarshine Hewavitharanage, Launa Steele, Isaac Dickenson; Visualization: Priyadarshine Hewavitharanage, Launa Steele, Isaac Dickenson; Funding acquisition: Priyadarshine Hewavitharanage; Supervision: Priyadarshine Hewavitharanage; Project Administration: Priyadarshine Hewavitharanage.

ORCID

Priyadarshine Hewavitharanage

 <https://orcid.org/0000-0001-8982-8733>

Launa Steele

 <https://orcid.org/0000-0001-6025-0544>

Isaac Dickenson

 <https://orcid.org/0000-0002-4434-6754>

References

- [1]. Hewavitharanage, P.; Warshawsky, R.; Rosokha, S. V.; Vaal, J.; Stickler, K.; Bachynsky, D.; Jairath, N. *Tetrahedron* **2020**, *76* (42), 131515–131525.
- [2]. Barin, G.; Yilmaz, M. D.; Akkaya, E. U. *Tetrahedron Lett.* **2009**, *50* (15), 1738–1740.
- [3]. Sharma, R.; Gobeze, H. B.; D'Souza, F.; Ravikanth, M. *ChemPhysChem* **2016**, *17* (16), 2516–2524.
- [4]. Sapsford, K. E.; Berti, L.; Medintz, I. L. *Angew. Chem. Int. Ed Engl.* **2006**, *45* (28), 4562–4589.
- [5]. Förster, T. *Ann. Phys.* **1948**, *437* (1–2), 55–75.
- [6]. Dexter, D. L. *J. Chem. Phys.* **1953**, *21* (5), 836–850.
- [7]. Al-Omari, S. J. *Biol. Phys.* **2016**, *42* (3), 373–382.
- [8]. McConnell, H. M. *J. Chem. Phys.* **1961**, *35* (2), 508–515.
- [9]. Pourtois, G.; Beljonne, D.; Cornil, J.; Ratner, M. A.; Brédas, J. L. *J. Am. Chem. Soc.* **2002**, *124* (16), 4436–4447.
- [10]. *Principles of Fluorescence Spectroscopy*; Lakowicz, J. R., Ed.; Springer US: Boston, MA, 2006.
- [11]. Bhuckory, S.; Kays, J. C.; Dennis, A. M. *Biosensors (Basel)* **2019**, *9* (2), 76–111.
- [12]. Chen, G.; Song, F.; Xiong, X.; Peng, X. *Ind. Eng. Chem. Res.* **2013**, *52* (33), 11228–11245.
- [13]. Rainey, K. H.; Patterson, G. H. *Proc. Natl. Acad. Sci. U. S. A.* **2019**, *116* (3), 864–873.
- [14]. Zohoorian-Abootorabi, T.; Sane, H.; Iranfar, H.; Saberi, M. R.; Chamani, J. *Spectrochim. Acta A Mol. Biomol. Spectrosc.* **2012**, *88*, 177–191.
- [15]. Blouin, S.; Craggs, T. D.; Lafontaine, D. A.; Penedo, J. C. *Methods Mol. Biol.* **2009**, *543*, 475–502.
- [16]. Gustiananda, M.; Liggins, J. R.; Cummins, P. L.; Gready, J. E. *Biophys. J.* **2004**, *86* (4), 2467–2483.
- [17]. Yang, J.; Chen, H.; Vlahov, I. R.; Cheng, J.-X.; Low, P. S. *Proc. Natl. Acad. Sci. U. S. A.* **2006**, *103* (37), 13872–13877.
- [18]. Liu, Y.; Yang, G.; Jin, S.; Zhang, R.; Chen, P.; Tengjisi; Wang, L.; Chen, D.; Weitz, D. A.; Zhao, C.-X. *Angew. Chem. Int. Ed Engl.* **2020**, *59* (45), 20065–20074.
- [19]. Yuan, L.; Lin, W.; Zheng, K.; Zhu, S. *Acc. Chem. Res.* **2013**, *46* (7), 1462–1473.
- [20]. Hu, R.; Zhang, X.; Zhao, Z.; Zhu, G.; Chen, T.; Fu, T.; Tan, W. *Angew. Chem. Int. Ed Engl.* **2014**, *53* (23), 5821–5826.
- [21]. Rajdev, P.; Ghosh, S. J. *Phys. Chem. B* **2019**, *123* (2), 327–342.
- [22]. Saxena, S.; Pradeep, A.; Jayakannan, M. *ACS Appl. Bio Mater.* **2019**, *2* (12), 5245–5262.
- [23]. Benniston, A. C.; Copley, G. *Phys. Chem. Chem. Phys.* **2009**, *11* (21), 4124–4131.
- [24]. Karolin, J.; Johansson, L. B.-A.; Strandberg, L.; Ny, T. *J. Am. Chem. Soc.* **1994**, *116* (17), 7801–7806.
- [25]. Ziessel, R.; Ulrich, G.; Harriman, A. *New J Chem* **2007**, *31* (4), 496–501.
- [26]. Ulrich, G.; Ziessel, R.; Harriman, A. *Angew. Chem. Int. Ed Engl.* **2008**, *47* (7), 1184–1201.
- [27]. Patalag, L. J.; Hoche, J.; Holzapfel, M.; Schmiedel, A.; Mitric, R.; Lambert, C.; Werz, D. B. *J. Am. Chem. Soc.* **2021**, *143* (19), 7414–7425.
- [28]. Hewavitharanage, P.; Nzeata, P.; Wiggins, J. *Eur. J. Chem.* **2012**, *3* (1), 13–16.
- [29]. Delmotte, C.; Delmas, A. *Bioorg. Med. Chem. Lett.* **1999**, *9* (20), 2989–2994.
- [30]. Laia, C. A. T.; Costa, S. M. B. *Chem. Phys. Lett.* **1998**, *285* (5–6), 385–390.
- [31]. Che, W.; Zhang, L.; Li, Y.; Zhu, D.; Xie, Z.; Li, G.; Zhang, P.; Su, Z.; Dou, C.; Tang, B. Z. *Anal. Chem.* **2019**, *91* (5), 3467–3474.
- [32]. Hu, W.; Ma, H.; Hou, B.; Zhao, H.; Ji, Y.; Jiang, R.; Hu, X.; Lu, X.; Zhang, L.; Tang, Y.; Fan, Q.; Huang, W. *ACS Appl. Mater. Interfaces* **2016**, *8* (19), 12039–12047.
- [33]. Swider, E.; Maharjan, S.; Houkes, K.; van Riessen, N. K.; Figdor, C.; Srinivas, M.; Tagit, O. *ACS Appl. Bio Mater.* **2019**, *2* (3), 1131–1140.
- [34]. Adams, P. G.; Collins, A. M.; Sahin, T.; Subramanian, V.; Urban, V. S.; Vairaprakash, P.; Tian, Y.; Evans, D. G.; Shreve, A. P.; Montano, G. A. *Nano Lett.* **2015**, *15* (4), 2422–2428.
- [35]. Galvao, J.; Davis, B.; Tilley, M.; Normando, E.; Duchon, M. R.; Cordeiro, M. F. *FASEB J.* **2014**, *28* (3), 1317–1330.
- [36]. Takayama, R.; Inoue, Y.; Murata, I.; Kanamoto, I. *Colloids interfaces* **2020**, *4* (3), 28.
- [37]. Hewavitharanage, P. *Eur. J. Chem.* **2012**, *3* (4), 395–398.
- [38]. Warshawsky, R.; Vaal, J.; Hewavitharanage, P. *Eur. J. Chem.* **2017**, *8* (4), 321–327.



Copyright © 2021 by Authors. This work is published and licensed by Atlanta Publishing House LLC, Atlanta, GA, USA. The full terms of this license are available at <http://www.eurjchem.com/index.php/eurjchem/pages/view/terms> and incorporate the Creative Commons Attribution-Non Commercial (CC BY NC) (International, v4.0) License (<http://creativecommons.org/licenses/by-nc/4.0>). By accessing the work, you hereby accept the Terms. This is an open access article distributed under the terms and conditions of the CC BY NC License, which permits unrestricted non-commercial use, distribution, and reproduction in any medium, provided the original work is properly cited without any further permission from Atlanta Publishing House LLC (European Journal of Chemistry). No use, distribution or reproduction is permitted which does not comply with these terms. Permissions for commercial use of this work beyond the scope of the License (<http://www.eurjchem.com/index.php/eurjchem/pages/view/terms>) are administered by Atlanta Publishing House LLC (European Journal of Chemistry).